European Radiology (2019) 29:1703–1713
https://doi.org/10.1007/s00330-018-5778-3

CHEST

The "solid" component within subsolid nodules: imaging definition, display, and correlation with invasiveness of lung adenocarcinoma, a comparison of CT histograms and subjective evaluation

WenTing Tu[1] · ZhaoBin Li[2] · Yun Wang[1] · Qiong Li[1] · Yi Xia[1] · Yu Guan[1] · Yi Xiao[1] · Li Fan[1] · ShiYuan Liu[1]

Received: 28 May 2018 / Revised: 21 August 2018 / Accepted: 19 September 2018 / Published online: 15 October 2018

Abstract

Objective To validate three proposed definitions of the "solid" component of subsolid nodules, as compared to CT histograms and the use of different window settings, for discriminating the invasiveness of adenocarcinomas in a manner that facilitates routine clinical assessment.

Methods We retrospectively analyzed 328 pathologically confirmed lung adenocarcinomas, manifesting as subsolid nodules. Three-dimensional CT histograms were generated by setting 11 CT attenuation intervals from -400 to 50 HU, at 50 HU intervals, and the voxel percentage within each CT attenuation interval was generated automatically. Three definitions of the "solid" component were proposed, and 10 medium window settings were set to evaluate the "solid" component. The diagnostic performance of the three definitions for identifying invasive adenocarcinoma was compared with that of CT histogram analysis and subjective evaluation with medium window settings.

Results A parallel diagnosis using five intervals with the largest AUC (AUC ≥ 0.797) demonstrated good differential diagnostic performance, with 78% sensitivity and 73.7% specificity. Definition 2 (visibility in the mediastinum window) yielded higher accuracy (75.6%) than the other two definitions ($p < 0.01$). A medium window setting of -50 WL/2 WW gave a larger AUC than the other nine medium window settings as well as definition 2, with 82.5% specificity and 88.5% PPV, which was higher than those of parallel diagnosis with CT histogram and definition 2.

Conclusion Using -50 WL/2 WW is the optimum approach for evaluating the "solid" component and discriminating invasiveness, superior to using 3D CT histograms and definition 2, and convenient in routine clinical assessment.

Key Points

- *-50 WL/2 WW gave a larger AUC than definition 2.*
- *The specificity of -50 WL/2 WW was higher than CT histograms.*
- *-50 WL/2 WW offers the best evaluation of the solid component.*

Keywords Lung · Adenocarcinoma · Solitary pulmonary nodule · Tomography, X-ray computed

WenTing Tu and ZhaoBin Li contributed equally to this work.

Electronic supplementary material The online version of this article (https://doi.org/10.1007/s00330-018-5778-3) contains supplementary material, which is available to authorized users.

✉ Li Fan
fanli0930@163.com

✉ ShiYuan Liu
lsy0930@163.com

[1] Department of Radiology, Changzheng Hospital, Second Military Medical University, No. 415 Fengyang Road, Shanghai 200003, China

[2] Department of Radiation Oncology, Shanghai Jiao Tong University Affiliated Sixth People's Hospital, Shanghai 200233, China

Abbreviations

AAH	Atypical adenomatous hyperplasia
AIS	Adenocarcinoma in situ
AUC	Area under the curve
CT	Computed tomography
DFS	Disease-free survival
GGNs	Ground-glass nodules
IAC	Invasive adenocarcinoma
IASLC/ATS/ERS	International Association for the Study of Lung Cancer/American Thoracic Society/European Respiratory Society
LW	Lung window
MIA	Minimally invasive adenocarcinoma

MW	Mediastinal window
NPV	Negative predictive value
NSNs	Nonsolid nodules
NRI	Net reclassification improvement
OR	Odds ratio
PSNs	Part-solid nodules
PPV	Positive predictive value
ROC	Receiver operating characteristic

Introduction

With the global increase in lung cancer screening by low-dose computed tomography (CT), the detection of subsolid nodules is escalating. Most early-stage lung cancers are adenocarcinomas and manifest as subsolid nodules on thin-slice CT [1]. Subsolid nodules are classified into part-solid nodules (PSNs) and nonsolid nodules (NSNs). The difference between PSN and NSN lies in the presence of solid components within the nodule [2]. The correct recognition of a solid component within subsolid nodules is essential for the classification, management, determination of invasion, and prediction of prognosis of these nodules. It has been reported that the invasiveness of adenocarcinoma is related to the solid components [3–5]. According to the classification system proposed by IASLC/ATS/ERS in 2011 [6], lung adenocarcinoma is classified into pre-invasive adenocarcinoma (i.e., atypical adenomatous hyperplasia [AAH] and adenocarcinoma in situ [AIS]), minimally invasive adenocarcinoma (MIA), and invasive adenocarcinoma (IAC). The 5-year disease-free survival (DFS) in AIS and MIA is 100%, which is significantly higher than that in IAC (range 38–86%, $p < 0.001$), depending on the predominant histologic subtype [7–9]. Due to the excellent prognosis of MIA, pre-invasive adenocarcinoma and MIA have been considered to be non-invasive lesions in some studies [10].

It has been reported that solid components could be viewed using different CT window settings [2, 11–15], such as lung window (LW) settings, mediastinal window (MW) settings, or medium window settings, but there is still no consensus about the appropriate window settings for displaying solid components. A large comparison study on ground-glass nodules (GGNs) and their pathologic invasiveness has previously been proposed to conduct with the use of different window settings and quantitative density analysis [16]. Density histogram analysis is the optimal modality for quantitative density analysis. The pixel volume proportion within a density interval may help to identify the homogeneity of subsolid nodules. However, the subjective evaluation with different CT window settings is easy and simple in routine clinical assessment. Until now, there are rare studies about the comprehensive comparison between different window settings and CT histogram attenuation interval analysis on the aspect of solid component in a large sample size. Based on the previous studies, three definitions of "solid" component of subsolid nodules were proposed in this study.

Therefore, the present study sought to compare the diagnostic accuracy of three proposed definitions of the "solid" component of subsolid nodules, then to be compared with the CT histograms and different medium window settings in terms of the ability to discriminate the invasiveness of adenocarcinomas comprehensively, and to facilitate routine clinical investigations.

Material and methods

Patient population

From January 2011 to December 2015, 344 consecutive patients with lung cancer manifesting as subsolid nodules were admitted to the same hospital for surgery. The inclusion criteria were as follows: no previous treatment history; pulmonary adenocarcinoma confirmed by surgical pathology; a lesion manifesting as a subsolid nodule on thin-slice (≤ 1-mm) CT images; availability of complete thin-slice images reconstructed using a standard algorithm in Digital Imaging and Communications in Medicine (DICOM) format; no marked cavity, cysts, or other air-containing space. The exclusion criteria were non-adenocarcinoma; previous treatment; incomplete thin-slice images for reconstruction; and presence of a marked cavity, cysts, or other air-containing space. Among these patients, 2 patients with squamous cell carcinoma, 1 with small cell lung cancer, 11 without raw thin-slice images, and 2 with marked cysts were excluded. Thus, 328 patients (114 men, 214 women; age range, 27–80 years, mean age 56.45 ± 10.33 years) with 328 subsolid nodules (size range, 9~29 mm, mean size 18 mm ± 8 mm) were included (Fig. 1). In this retrospective study, pre-invasive and MIA were considered as non-invasive lesions [10]; there were 114 cases with non-invasive lesions (AAH and AIS, 56; MIA, 58) and 214 with IAC.

The study protocol was approved by the local ethics committee and the need to obtain informed consent was waived due to the retrospective nature of the study.

CT scanning

All patients underwent scanning on a 256-slice CT scanner or 128-slice CT scanner (Brilliance-iCT and

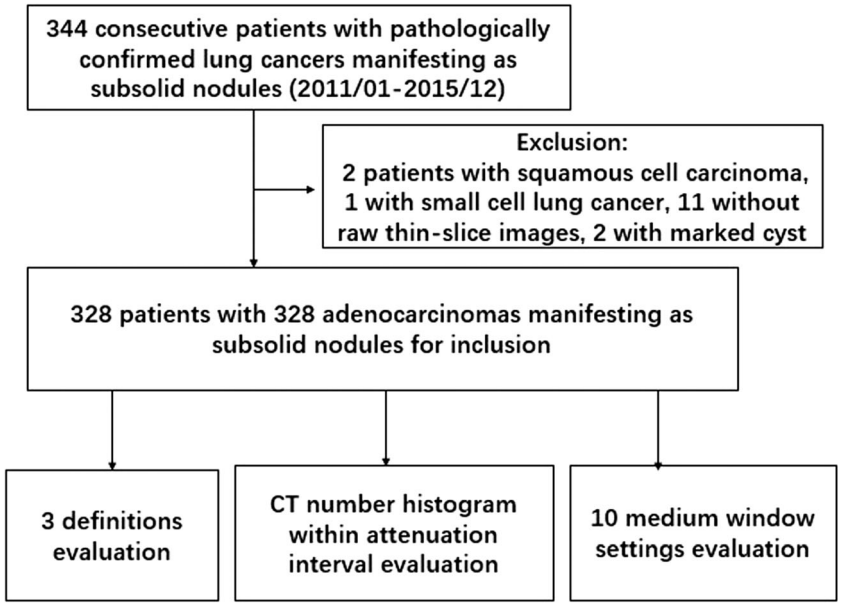

Fig. 1 Flowchart of study population

Ingenuity CT; Philips Healthcare). Breath-hold training was performed before each examination. All patients were asked to hold their breath at the end of inspiration. Unenhanced imaging was performed from the thoracic inlet to the middle portion of the kidneys. The following scanning parameters were used: slice thickness 1 mm, slice increment 1 mm, collimation 128 × 0.625 mm (iCT) or 64 × 0.625 mm (Ingenuity CT), rotation 0.5 s, pitch 0.8 (iCT) or 1.02 (Ingenuity CT), matrix 512 × 512, high- and standard-resolution algorithms, 120 kVp, and dose modulation ACS (iCT) or Z DOM (Ingenuity CT).

Image evaluation

3D CT number histogram analysis within given CT attenuation intervals

All raw thin-slice DICOM format images were transferred to a workstation (SW001.001version, United Imaging Healthcare) and postprocessed using the pulmonary nodule advanced analysis tool software. The nodules were segmented semi-automatically in LW settings (WW 1500, WL -500) using a standard algorithm, and the radiologist then adjusted the margin with manual drawing slice by slice on the axial, sagittal, and coronal planes to ensure more accurate segmentation. Ninety-seven of the included subsolid nodules were selected randomly and used to evaluate the reproducibility of intra-observer and inter-observer segmentation by two experienced thoracic radiologists with 3 years and 13 years of experience. The two radiologists were blinded to each other's segmentation. The thoracic radiologist with 3 years of experience segmented these 97 subsolid nodules twice within a 2-month interval for intra-observer consistency evaluation. The whole quantitative data set consisted of the segmentation of these first 97 subsolid nodules and the segmentation of the remaining 231 subsolid nodules by the radiologist with 3 years of experience.

After the segmentation, a series of quantitative parameters (volume, area, maximum diameter in the axial plane, minimum diameter in the axial plane, and minimum, maximum, and mean CT value) and a 3D CT number histogram could be generated automatically. An adjustable CT attenuation bar on the axial view displayed the voxel volume within any attenuation interval (Fig. 2c), and the voxel percentage was automatically generated. The subsolid nodule size was defined as the mean of maximum diameter and minimum diameter in the axial plane. In order to quantitate the voxel distribution within a given CT attenuation interval, 11 CT attenuation intervals were set, from -400 to 50 HU, with an interval of 50 HU, including < -400 HU and ≥ 50 HU. The voxel percentage within each CT attenuation interval was generated automatically and recorded.

Subjective evaluations with 10 medium window settings

The visibility of all subsolid nodules was evaluated by the thoracic radiologist with 10 years of experience, on 10 medium window settings: setting window width (WW) as 2, and window level (WL) as -400 HU, -350 HU, -300 HU, -250 HU, -200 HU, -150 HU, -100 HU, -50 HU, 0 HU, and 50 HU. The WL was the same as the CT histogram attenuation interval. The subsolid nodules were classified as visible or not visible, and the visible nodules were presumed to be IAC.

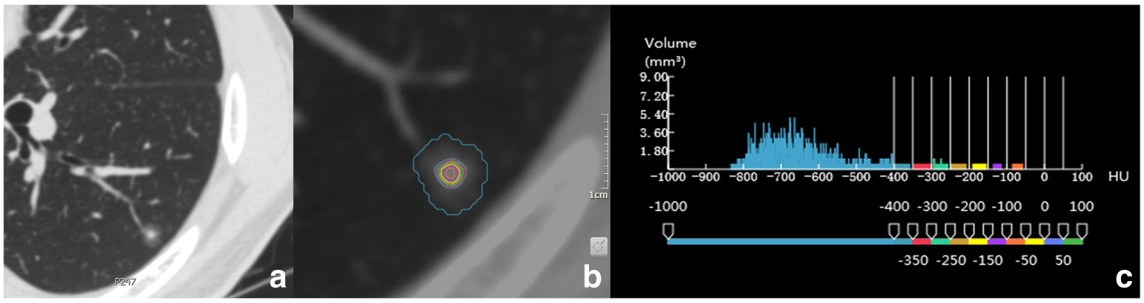

Fig. 2 CT number histogram analysis of non-invasive lesions (adenocarcinoma in situ). A 40-year-old male patient with adenocarcinoma in situ in the left lower lobe. **a** Lung window settings reveal heterogeneous subsolid nodule. **b** Color-coded pixel distribution in the subsolid nodule within different CT attenuation intervals. **c** 3D CT number histogram shows that the voxel percentage is 96%, 1%, 1%, 1%, 1%, 0%, 0%, 0%, 0%, 0%, and 0% within the < -400, -400 to -350, -350 to -300, -300 to -250, -250 to -200, -200 to -150, -150 to -100, -100 to -50, -50 to 0, 0 to 50, and ≥ 50 HU CT attenuation intervals, respectively

Evaluation of the three proposed definitions of "solid" components

According to recent reports and given the controversy about the solid component of subsolid nodules, we proposed three definitions for the solid components in this study. These were based on (1) the heterogeneity on LW setting, (2) the visibility of the subsolid nodules on MW settings, and (3) whether the maximum CT value of the subsolid nodule was higher than that of the vessel. Pathology findings were considered the golden standard.

For definition 1, the homogeneity of subsolid nodules were evaluated on routine LW settings (WW 1500, WL − 500), using a high-resolution algorithm, by two radiologists with 10 years and 5 years of experience in thoracic radiology. In cases of discrepancy, consensus was reached by consulting a third thoracic expert with 30 years of experience. The heterogeneity on LW setting was only based on the density of subsolid nodules, a single denser voxel. The vessels and bronchus in the subsolid nodules were excluded when evaluating the homogeneity of the subsolid nodules. On LW settings, subsolid nodules were classified as homogeneous or heterogeneous, and heterogeneous nodules were supposed to be IAC.

For definition 2, the visibility of the subsolid nodules was evaluated on routine MW settings (WW 350, WL 40), using a standard-resolution algorithm, by a thoracic radiologist with 10 years of experience. The vessels in the subsolid nodules were excluded when evaluating the visibility of the subsolid nodules. Subsolid nodules were classified as visible or not visible, and the visible nodules were supposed to be IAC.

For definition 3, the maximum CT values of the vessel and the subsolid nodule were compared to classify the subsolid nodules. The maximum CT value of the subsolid nodule was derived from 3D CT number histogram analysis. A region of interest (ROI) was drawn on the vessel adjacent to the subsolid nodule on LW settings using a standard algorithm, on the largest axial slice of the subsolid nodule, and the maximum CT value of the vessel was recorded. The ROI covered at least two thirds of the maximum axial region of the vessel. Subsolid nodules with a maximum CT value higher than that of the vessel were supposed to be IAC.

Statistical analysis

Statistical analyses were performed using SPSS 21.0 (IBM) and the R software (version 3.0.1; R Foundation for Statistical Computing; http://www.Rproject.org). The intra-class correlation coefficient (ICC) was used to evaluate segmentation variability. The degree of agreement was interpreted as follows: less than 0.20, poor agreement; 0.21–0.40, fair agreement; 0.41–0.60, moderate agreement; 0.61–0.80, substantial agreement; and 0.81–1.00, almost perfect agreement [17]. *t* test and receiver operating characteristic (ROC) curve analyses were used to compare quantitative parameters between non-invasive lesions and IAC. Variance analyses, Bonferroni tests, *t* tests, and ROC curve analyses were used to evaluate the voxel percentage within 11 CT attenuation intervals. For the subjective evaluation using different window settings, chi-square tests, logistic regression analyses, and ROC curve analyses were performed. The area under the curve (AUC), accuracy, sensitivity, specificity, positive predictive value (PPV), negative predictive value (NPV), and odds ratio (OR) were calculated. For the comparison between the three definitions and 10 medium window settings, the net reclassification improvement (NRI) was assessed. A two-sided p value < 0.05 was considered statistically significant.

Results

Intra-observer and inter-observer segmentation reproducibility

The intra-observer ICC of all the quantitative parameters, including volume, area, maximum and minimum diameter,

minimum, maximum, and mean CT value, were all greater than 0.81, indicating almost perfect agreement. The inter-observer ICC of the minimum CT value and minimum axial diameter showed substantial agreement (0.696 and 0.758, respectively), while the other parameters showed almost perfect agreement (ICC > 0.81) (Table 1).

3D CT number histogram within given CT attenuation intervals

There were statistically significant differences in voxel percentage within the 11 CT attenuation intervals between non-invasive lesions and IAC by *t* test ($p < 0.05$). The AUC of the ROC curve for discriminating non-invasive lesions from IAC is shown in Table 2. Five AUCs were equal or larger than 0.797 in the < -400 HU, -150 HU to -100 HU, -200 HU to -150 HU, -100 HU to -50 HU, and -50 HU to 0 HU CT attenuation intervals, which demonstrated good differential diagnostic performance. Within the < -400 HU interval, if the voxel percentage was less than the cutoff value, IAC was diagnosed. Within the other intervals, if the voxel percentages were more than the cutoff value, IAC was diagnosed. The cutoff values of the voxel percentage (sensitivity vs. specificity) were 84.5% (81.6% vs. 70.1%), 0.5% (77.6% vs. 78.1%), 1.5% (69.2% vs. 86%), 0.5% (72.4% vs. 82.5%), and 0.5% (68.7% vs. 86%) within the < -400 HU, -150 to -100 HU, -200 to -150 HU, -100 to -50 HU, and -50 to 0 HU CT attenuation intervals, respectively (Figs. 2, 3, and 4). The corresponding PPV and NPV are shown in Table 2. The PPV for diagnosis of non-invasive lesions in the < -400 HU interval was low, but the PPVs for diagnosing IAC of the other intervals exceeded 79%.

The five intervals with larger AUCs were selected to make a parallel diagnosis, setting IAC as positive and non-invasive lesions as negative. If one of the five intervals indicated a positive diagnosis, then the final diagnosis was positive. The AUC was 0.759, indicating good diagnostic performance. The accuracy, sensitivity, and specificity of this approach were 76.5%, 78%, and 73.7%, respectively. The sensitivity of parallel diagnosis was higher than most of the sensitivities of single intervals. The PPV and NPV were 84.8% and 64.1%, respectively.

Subjective evaluations: visibility on MW and 10 medium window settings

The visibility of non-invasive lesion was significantly less than that of IAC using MW settings and 10 medium window settings, based on chi-square tests ($p < 0.001$, Table 3, Fig. 5). The AUC of different window settings and logistic regression analysis results are shown in Table 3. The AUCs of five window settings were equal or larger than 0.743 (WW 2, WL -50, 0, -100, -150, and MW settings), while the accuracy of these five window settings was similar. The PPV and OR both increased with the increase of WL.

The NRIs between MW settings and the 10 other medium window settings are shown in Table 4. MW was significantly better than WL -400, WL -350, WL -300, and WL -200 in terms of the discrimination of IAC ($p < 0.05$). While WL -50 and WL -100 were superior to MW due to the negative NRI value, no significant difference was found between them. Considering all the parameters in Table 3, the optimum window settings for differential diagnosis were -50 WL and 2 WW, with a maximum AUC of 0.773, sensitivity of 72.2%, specificity of 82.5%, accuracy of 75.6%, PPV of 88.5%, NPV of 61%, and OR of 12.06, respectively.

Diagnostic performance of the three proposed definitions of solid components

The proposed definitions of solid components were regarded as reflecting IAC and were compared with the golden standard of pathological diagnosis. By definition 1, the ratio of heterogeneity in IAC (207/214, 96.73%) was significantly higher than that in non-invasive lesions (103/114, 90.35%) on LW settings ($\chi^2 = 5.834$, $p < 0.05$). By definition 2, the visibility of the nodule on MW settings was significantly higher in IAC (162/214, 75.70%) than in non-invasive lesions (28/114, 24.56%) ($\chi^2 = 79.813$, $p < 0.001$). By definition 3, the ratio of subsolid nodules with maximum attenuation higher than

Table 1 Intra-observer and inter-observer agreement for the quantitative parameters generated by manual segmentation

	Intra-observer			Inter-observer		
	ICC	95% CI	*p*	ICC	95% CI	*p*
Volume	0.997	0.996~0.998	< 0.001	0.935	0.592~0.977	< 0.001
Area	0.970	0.956~0.980	< 0.001	0.916	0.710~0.964	< 0.001
Maximum axial diameter	0.927	0.893~0.951	< 0.001	0.839	0.718~0.903	< 0.001
Minimum axial diameter	0.849	0.783~0.896	< 0.001	0.758	0.644~0.836	< 0.001
Maximum CT value	0.995	0.992~0.997	< 0.001	0.949	0.925~0.966	< 0.001
Minimum CT value	0.821	0.745~0.877	< 0.001	0.696	0.231~0.858	< 0.001
Average CT value	0.989	0.984~0.993	< 0.001	0.914	0.815~0.954	< 0.001

Table 2 ROC analysis of voxel percentage within different CT attenuation intervals for the differentiation IAC from non-invasive lesions

Attenuation interval	AUC	CI lower	CI upper	*p*	Sensitivity (%)	Specificity (%)	Accuracy (%)	Threshold (%)	PPV (%)	NPV (%)
< -400	0.816	0.712	0.830	0.000	81.6	70.1	74.1	84.500	59.2	87.7
-400~-350	0.727	0.633	0.782	0.000	68.7	69.3	68.9	3.500	80.8	54.1
-350~-300	0.558	0.454	0.657	0.000	81.8	61.4	74.7	1.500	79.9	64.2
-300~-250	0.778	0.669	0.802	0.000	78.5	71.9	76.2	1.500	84	64.1
-250~-200	0.789	0.682	0.815	0.000	73.4	80.7	75.9	1.500	80.8	66.1
-200~-150	0.801	0.673	0.806	0.000	69.2	86.0	75.0	1.500	90.2	59.8
-150~-100	0.808	0.682	0.808	0.000	77.6	78.1	77.7	0.500	86.9	65
-100~-50	0.797	0.689	0.809	0.000	72.4	82.5	75.9	0.500	88.6	61.4
-50~0	0.797	0.680	0.799	0.000	68.7	86.0	74.7	0.500	90.2	59.4
0-50	0.768	0.655	0.777	0.000	59.8	91.2	70.7	0.500	92.8	54.7
> 50	0.647	0.567	0.703	0.002	33.6	94.7	54.9	0.500	92.3	43.2

CI confidence interval, *PPV* positive predicted value, *NPV* negative predicted value

that of vessels in LW settings was significantly greater for IAC (122/214, 57.01%) than for non-invasive lesions (22/114,19.30%) ($\chi^2 = 42.949$, $p < 0.001$). Table 5 shows the diagnostic performance of the three proposed definitions. Definition 2 had the highest accuracy (75.6%), PPV (85.3%), NPV (62.3%), and OR (9.57) and had moderate sensitivity (75.7%) and specificity (75.43%). Table 4 shows that definition 2 was significantly better than definitions 1 and 3 (NRI 0.45 and 0.13, respectively; $p < 0.05$). Therefore, of the three proposed definitions, definition 2 was superior for depicting solid components.

Cross-classification of subsolid nodules using the three definitions

For homogeneous subsolid nodules, the visibility on MW settings was not different between non-invasive lesions and IAC (0% vs. 28.57%, $\chi^2 = 1.235$, $p = 0.267$). However, for the nodules visible on MW settings, significantly more nodules were heterogeneous among IAC (160/207, 77.29%) than among non-invasive lesions (28/103, 27.18%) ($\chi^2 = 72.361$, $p < 0.001$). For both visible and non-visible subsolid nodules on MW settings, homogeneity on LW settings was not different between non-invasive lesions and IAC ($p = 1.00$, $p = 0.572$, respectively). For heterogeneous subsolid nodules, the sensitivity, specificity, accuracy, PPV, and NPV when using definition 2 to diagnose IAC were 77.3%, 72.8%, 75.8%, 85.1%, and 61.5%, respectively (Supplemental Table S1).

For subsolid nodules with a maximum attenuation higher than that of the vessels, the sensitivity, specificity, accuracy, PPV, and NPV when using definition 1 to diagnose IAC was 99.2%, 0.0%, 84.0%, 84.6%, and 0.0%, respectively (Supplemental Table S2). While using definition 2, the sensitivity, specificity, accuracy, PPV, and NPV were 93.4%, 25.0%, 83.3%, 87.7%, and 42.9%, respectively (Supplemental Table S3). For both subsolid nodules with a maximum attenuation higher or lower than that of the vessels, there was no difference in the homogeneity on LW settings ($p = 1.00$, $p = 0.203$, respectively; Supplement Table S2), but the visibility on MW settings differed significantly between non-invasive lesion and IAC ($p < 0.05$, $p < 0.001$, respectively; Supplemental Table S3), indicating the MW setting may play a greater role in the discrimination of IAC.

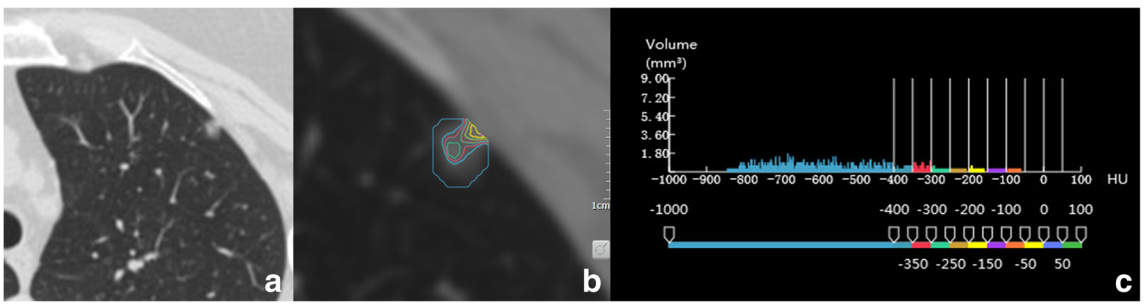

Fig. 3 CT number histogram analysis of non-invasive lesion (minimally invasive adenocarcinoma). A 62-year-old female patient with minimally invasive adenocarcinoma in the left upper lobe. **a** Lung window settings reveal heterogeneous subsolid nodule. **b** Color-coded pixel distribution in the subsolid nodule within different CT attenuation intervals. **c** 3D CT number histogram shows that the voxel percentage is 85%, 5%, 5%, 3%, 1%, 1%, 0%, 0%, 0%, 0%, and 0% within the 11 CT attenuation intervals indicated in Fig. 2, respectively

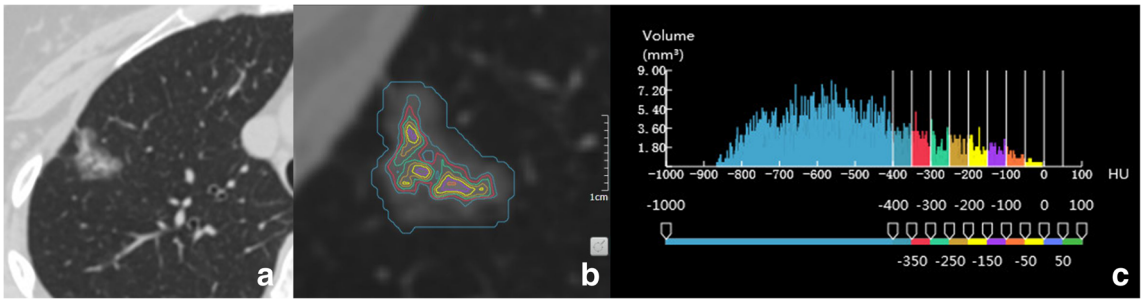

Fig. 4 CT number histogram analysis of invasive adenocarcinoma. A 36-year-old female patient with invasive adenocarcinoma in the right upper lobe. **a** Lung window settings reveal heterogeneous subsolid nodule. **b** Color-coded pixel distribution in the subsolid nodule within different CT attenuation intervals. **c** 3D CT number histogram shows that the voxel percentage is 75%, 6%, 5%, 4%, 3%, 3%, 3%, 1%, 0%, 0%, and 0% within the 11 CT attenuation intervals indicated in Fig. 2, respectively

Discussion

In this study, three definitions of "solid" components of subsolid nodules were defined and validated against the invasiveness of adenocarcinoma, based on a comparison of 3D CT histogram attenuation interval analysis and different medium window settings for the discrimination of IAC from non-invasive lesions.

Pathologically, the solid component represents alveolar collapse and intra-tumoral fibrosis, which is associated with tumor invasiveness and prognosis [18]. Many studies have focused on measurement of the solid component. The CT number histogram has been reported as the most common quantitative indicator for evaluating the invasiveness of adenocarcinoma [19–21]. However, most of these studies focused on the CT attenuation threshold to predict invasiveness. Few studies have considered the attenuation interval characteristics of the histogram. The present study evaluated the pixel volume percentage distribution of subsolid nodules within different attenuation intervals. The histogram-based CT attenuation threshold for predicting the invasiveness of adenocarcinoma varied: -300 HU, -194 HU, etc. [4, 22–24]. Therefore, we set an attenuation threshold from -400 HU, using an interval of 50 HU, to evaluate the difference in the pixel distribution within the given intervals. There was a significant difference in pixel volume percentage between non-invasive lesion and IAC in each interval. Moreover, with the increase in CT attenuation, the specificity of prediction of IAC increased, which was consistent with the pathological basis of IAC, which has more solid components. Kamiya et al [25] found that a solid volume of greater than 0 HU could predict the prognosis of patients with PSNs accurately. In this study, the volume percentage was used to predict invasiveness. The cutoff value of the volume percentage was 0.5% for both the -50 HU to 0 HU and 0 HU to 50 HU interval, respectively. The parallel diagnostic performance of five attenuation intervals with larger AUCs was good, with an accuracy of 76.5%, sensitivity of 78%, and specificity of 73.7%.

Some studies have suggested the use of a medium window, such as -160 HU, as the "solid" window setting [22, 26]. In order to compare with the quantitative CT histogram interval evaluation, a series of 10 window levels were set, from -400

Table 3 Visibility comparison between non-invasive lesions and IAC in different window settings

Window settings (WL, WW)	VR of "non-invasive" (%)	VR of IAC (%)	*p*	AUC	Sensitivity (%)	Specificity (%)	Accuracy (%)	PPV (%)	NPV (%)	OR	CI lower	CI upper
-400, 2	64.9	90.1	0.000	0.626	90.1	35.1	71.0	72.3	65.6	4.97	2.75	8.98
-350, 2	60.5	89.2	0.000	0.643	89.2	39.5	72.0	73.5	66.2	5.42	3.05	9.60
-300, 2	57	88.2	0.000	0.656	88.2	43.0	72.6	74.4	66.2	5.70	3.26	9.96
-250, 2	48.2	85.9	0.000	0.688	85.8	51.8	74.1	77.0	66.3	6.58	3.86	11.21
-200, 2	41.2	84.5	0.000	0.716	84.4	58.8	75.6	79.4	67.0	7.82	4.62	13.23
-150, 2	32.5	81.2	0.000	0.743	81.1	67.5	76.5	82.5	65.8	9.05	5.37	15.25
-100, 2	23.7	75.6	0.000	0.759	75.5	76.3	75.9	85.7	62.6	10.04	5.89	17.10
-50, 2	17.5	71.8	0.000	0.773	72.2	82.5	75.6	88.5	61.0	12.06	6.84	21.28
0, 2	11.4	63.4	0.000	0.761	63.7	88.6	72.3	91.3	56.4	13.55	7.13	25.72
50, 2	4.4	50.2	0.000	0.730	50.5	95.6	66.2	95.6	50.7	22.21	8.71	56.61
40, 350 (MW)	24.6	75.6	0.000	0.755	75.5	75.4	75.6	85.3	62.3	9.57	5.64	16.23

VR visibility rate, *MW* mediastinum window, *OR* odds ratio, *PPV* positive predicted value, *NPV* negative predicted value, *CI* confidence interval

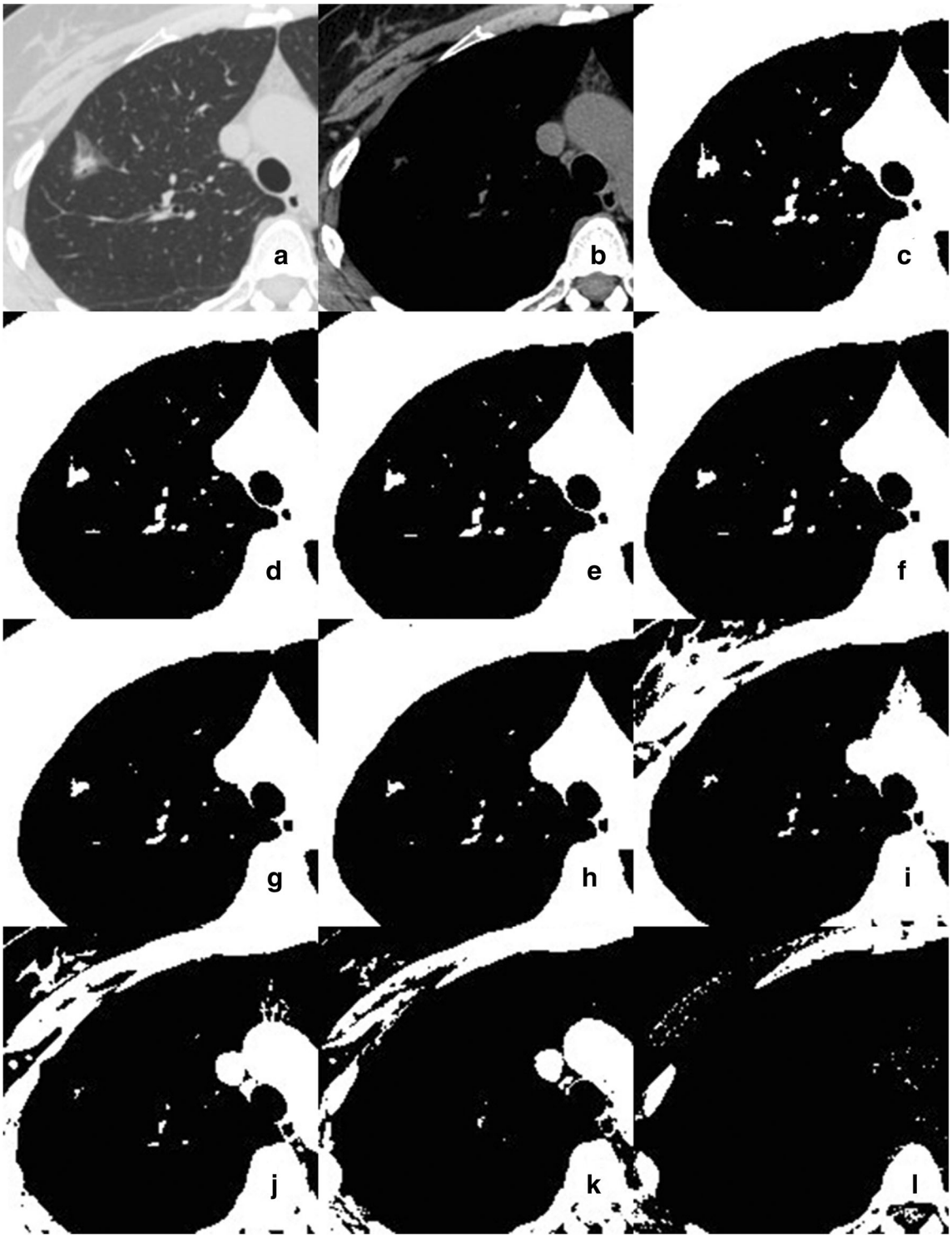

Fig. 5 Different window settings for invasive adenocarcinoma. A 36-year-old female patient with invasive adenocarcinoma in the right upper lobe. **a** Lung window (-500 WL/1500 WW). **b** Mediastinum window (40 WL/350 WW). **c** -400 WL/2 WW. **d** -350 WL/2 WW. **e** -300 WL/2 WW. **f** -250 WL/2 WW. **g** -200 WL/2 WW. **h** -150 WL/2 WW. **i** -100 WL/2 WW. **j** -50 WL/2 WW. **k** 0 WL/2 WW. **l** 50 WL/2 WW. The subsolid nodule is visible with the increase in WL to − 50 HU (**j**)

to 50 HU, with 50 HU intervals, to evaluate the visibility of subsolid nodules. Even with the lowest threshold (-400 WL/2 WW) for visual assessment, 9.9% of invasive disease was missed (Table 3). With the increase in the window level, the specificity and PPV increased. Tables 3 and 4 show that -50 WL/2 WW was the optimal setting, with a maximum AUC, as compared with other medium windows and the MW; the specificity and PPV were 82.5% and 88.5%, respectively, which

Table 4 Comparison of diagnostic performance of different methods with NRI

Methods	NRI	*p* value
Definition 2 vs. medium windows settings		
Definition 2 vs. WL -400, WW 2	0.26	< 0.0001
Definition 2 vs. WL -350, WW 2	0.22	0.0001
Definition 2 vs. WL -300, WW 2	0.20	0.0004
Definition 2 vs. WL -250, WW 2	0.13	0.004
Definition 2 vs. WL -200, WW 2	0.08	0.0419
Definition 2 vs. WL -150,WW 2	0.02	0.2633
Definition 2 vs. WL -100, WW 2	-0.01	0.3553
Definition 2 vs. WL -50, WW 2	-0.03	0.1483
Definition 2 vs. WL 0, WW 2	-0.01	0.404
Definition 2 vs. WL 50, WW 2	0.05	0.1758
The three proposed definitions		
Definition 2 vs. definition 1	0.45	< 0.0001
Definition 2 vs. definition 3	0.13	0.0043
Definition 3 vs. definition 1	0.31	0.0003

NRI net reclassification improvement

were higher than those values of parallel diagnosis with the CT histogram. Thus, using -50 WL/2 WW settings is superior to using a CT histogram and MW.

Additionally, there are still controversies about the routine LW and MW to use for evaluation of solid components. Initially, solid components within subsolid nodules were defined as those that completely obscured the lung parenchyma [2] or underlying lung architecture [11]. According to these definitions, the solid component should be viewed using LW settings. Therefore, we based definition 1 on the heterogeneity observed in LW settings, while definition 3 reflected the maximum CT attenuation of the subsolid nodules (higher than that of the lung vessels), based on obscuring the underlying lung architecture. The consolidation/tumor ratio (CTR) on LW settings has also been reported for evaluating invasiveness and prognosis [27–29]. Matsunaga et al classified PSNs into ground glass-predominant and consolidation-predominant PSNs according to the CTR and proved that this classification was related to prognosis and treatment strategies [27]. However, the Fleischer Society recommended defining the size of a solid component in a PSN with MW settings [11]. Bak et al [15] defined a solid component as the portion detected in MW settings. Therefore, we based definition 2 on the visibility in MW settings. These three definitions were compared in terms of the frequency of solid components, to discriminate IAC using NRI. As shown in Tables 4 and 5, definition 2 was the optimum definition for depicting solid components. Supplemental Table S1 shows the cross-evaluation of heterogeneity on LW and visibility on MW. Only under the three definition circumstances, we suggested that subsolid nodules should be classified into PSNs and NSNs with MW, then NSNs reclassified into homogeneous and heterogeneous NSNs with LW settings in routine subjective evaluation of clinical work.

The CT number histogram attenuation interval analysis displays the pixel distribution and heterogeneity of subsolid nodules clearly. This analysis is quantitative, while the specificity and PPV of the parallel diagnosis was lower than that of the subjective evaluation using -50 WL/2 WW, indicating that using -50 WL/2 WW would be better for evaluating solid components. It is also more convenient to use this approach in a clinical setting, as compared to quantitative CT histogram analysis, which requires semi-automated segmentation of subsolid nodules, although the intra-observer and inter-observer segmentation showed substantial or almost perfect agreement.

There are several limitations in this study. First, the quantitative parameters were derived from the results of semi-automated segmentation. Small internal vessels and bronchi could not be excluded, which may affect the attenuation of the subsolid nodule. Second, 3D tumor segmentation is a complex and time-consuming process. Third, definition 1 of the solid component involves a subjective assessment of homogeneity, although consensus was ensured by consulting a third experienced expert. Fourth, there was no comparison of the pathology of the invasive solid component; rather, we focused only on the radiological definition and comparison. Further accurate comparisons should therefore be made in a future study.

In conclusion, our results suggest that the use of -50 WL/2 WW should be recommended for evaluating the solid components of subsolid nodules and for discriminating their invasiveness. This approach performs better than definition 2,

Table 5 Comparison of the three proposed definitions for the diagnosis of IAC

	"PSN" (*n*)	"NSN" (*n*)	Sensitivity (%)	Specificity (%)	Accuracy (%)	PPV (%)	NPV (%)	OR	CI lower	CI upper
Definition 1	207	7	96.73	9.65	66.5	66.8	61.1	3.16	1.19	8.39
Definition 2	162	52	75.70	75.44	75.6	85.3	62.3	9.57	5.64	16.23
Definition 3	122	92	57.01	80.70	65.2	84.7	50.0	5.55	3.24	9.50

Definition 1: "solid" component was regarded as the heterogeneity on LW settings. Definition 2: "solid" component was regarded as the visibility on MW settings. Definition 3: "solid" component was regarded as the maximum CT value of GGN was higher than that of vessels

OR odds ratio, *PPV* positive predicted value, *NPV* negative predicted value, *CI* confidence interval

which performed the best among the three proposed definitions, and CT histogram quantitative analysis, and is more convenient to use in routine clinical assessments.

Acknowledgements We would like to thank the assistance of the United Imaging Healthcare Co. Ltd. for the pulmonary nodule advanced analysis tool software development and technical support.

Funding This study has received funding from the National Key R&D Program of China (grant number 2016YFE0103000, 2017YFC1308703), the National Natural Science Foundation of China (grant number 81871321, 81370035), and the Youth Fund of the National Natural Science Foundation of China (grant number 81501618, 81501470).

Compliance with ethical standards

Guarantor The scientific guarantor of this publication is Prof. Li Fan.

Conflict of interest The authors of this manuscript declare no relationships with any companies, whose products or services may be related to the subject matter of the article.

Statistics and biometry Prof. Jian Lu (Department of Statistics, Second Military Medical University) kindly provided statistical advice for this manuscript.

Informed consent Written informed consent was waived by the Institutional Review Board.

Ethical approval An Institutional Review Board approval was obtained.

Methodology
- Retrospective
- Diagnostic or prognostic study
- Performed at one institution

References

1. Goo JM, Park CM, Lee HJ (2011) Ground-glass nodules on chest CT as imaging biomarkers in the management of lung adenocarcinoma. AJR Am J Roentgenol 196:533–543
2. Kim HY, Shim YM, Lee KS, Han J, Yi CA, Kim YK (2007) Persistent pulmonary nodular ground-glass opacity at thin-section CT: histopathologic comparisons. Radiology 245(1):267–275
3. Ding H, Shi J, Zhou X et al (2017) Value of CT characteristics in predicting invasiveness of adenocarcinoma presented as pulmonary ground-glass nodules. Thorac Cardiovasc Surg 65:136–141
4. Shikuma K, Menju T, Chen F et al (2016) Is volumetric 3-dimensional computed tomography useful to predict histological tumour invasiveness? Analysis of 211 lesions of cT1N0M0 lung adenocarcinoma. Interact Cardiovasc Thorac Surg 22:831–838
5. Yanagawa M, Johkoh T, Noguchi M et al (2017) Radiological prediction of tumor invasiveness of lung adenocarcinoma on thin-section CT. Medicine (Baltimore) 96:e6331
6. Travis WD, Brambilla E, Noguchi M et al (2011) International Association for the Study of Lung Cancer/American Thoracic Society/European Respiratory Society international multidisciplinary classification of lung adenocarcinoma. J Thorac Oncol 6:244–285
7. Yanagawa N, Shiono S, Abiko M, Ogata SY, Sato T, Tamura G (2013) New IASLC/ATS/ERS classification and invasive tumor size are predictive of disease recurrence in stage I lung adenocarcinoma. J Thorac Oncol 8:612–618
8. Yoshiya T, Mimae T, Tsutani Y et al (2016) Prognostic role of subtype classification in small-sized pathologic N0 invasive lung adenocarcinoma. Ann Thorac Surg 102:1668–1673
9. Luo J, Huang Q, Wang R et al (2016) Prognostic and predictive value of the novel classification of lung adenocarcinoma in patients with stage IB. J Cancer Res Clin Oncol 142:2031–2040
10. Fan L, Fang M, Li Z et al (2018) Radiomics signature: a biomarker for the preoperative discrimination of lung invasive adenocarcinoma manifesting as a ground-glass nodule. Eur Radiol. https://doi.org/10.1007/s00330-018-5530-z
11. Naidich DP, Bankier AA, MacMahon H et al (2013) Recommendations for the management of subsolid pulmonary nodules detected at CT: a statement from the Fleischner Society. Radiology 266:304–317
12. Kakinuma R, Muramatsu Y, Kusumoto M et al (2015) Solitary pure ground-glass nodules 5 mm or smaller: frequency of growth. Radiology 276:873–882
13. Godoy MC, Naidich DP (2009) Subsolid pulmonary nodules and the spectrum of peripheral adenocarcinomas of the lung: recommended interim guidelines for assessment and management. Radiology 253:606–622
14. Kim H, Park CM, Woo S et al (2013) Pure and part-solid pulmonary ground-glass nodules: measurement variability of volume and mass in nodules with a solid portion less than or equal to 5 mm. Radiology 269:585–593
15. Bak SH, Lee HY, Kim JH et al (2016) Quantitative CT scanning analysis of pure ground-glass opacity nodules predict further CT scanning change. Chest 149:180–191
16. Fan L, Li Q, Xiao Y, Wang Y, Liu SY (2016) How to define and display solid components within ground-glass nodules and differentiate pure ground-glass nodules from mixed ground-glass nodules? Radiology 281:325–326
17. Landis JR, Koch GG (1977) The measurement of observer agreement for categorical data. Biometrics 33:159–174
18. Maeshima AM, Niki T, Maeshima A, Yamada T, Kondo H, Matsuno Y (2002) Modified scar grade: a prognostic indicator in small peripheral lung adenocarcinoma. Cancer 95:2546–2554
19. Peng M, Li Z, Hu H et al (2016) Pulmonary ground-glass nodules diagnosis: mean change rate of peak CT number as a discriminative factor of pathology during a follow-up. Br J Radiol 89:20150556
20. Li Q, Fan L, Cao ET, Li QC, Gu YF, Liu SY (2017) Quantitative CT analysis of pulmonary pure ground-glass nodule predicts histological invasiveness. Eur J Radiol 89:67–71
21. Alpert JB, Rusinek H, Ko JP et al (2017) Lepidic predominant pulmonary lesions (LPL): CT-based distinction from more invasive adenocarcinomas using 3D volumetric density and first-order CT texture analysis. Acad Radiol 24:1604–1611
22. Yoshida Y, Sakamoto M, Maeda E et al (2015) Can image analysis on high-resolution computed tomography predict non-invasive growth in adenocarcinoma of the lung? Ann Thorac Cardiovasc Surg 21:8–13
23. Okada T, Iwano S, Ishigaki T et al (2009) Computer-aided diagnosis of lung cancer: definition and detection of ground-glass opacity type of nodules by high-resolution computed tomography. Jpn J Radiol 27:91–99
24. Cohen JG, Goo JM, Yoo RE et al (2016) Software performance in segmenting ground-glass and solid components of subsolid nodules in pulmonary adenocarcinomas. Eur Radiol 26:4465–4474
25. Kamiya S, Iwano S, Umakoshi H et al (2018) Computer-aided volumetry of part-solid lung cancers by using CT: solid component size predicts prognosis. Radiology 14:172319

26. Matsuguma H, Nakahara R, Anraku M et al (2004) Objective definition and measurement method of ground-glass opacity for planning limited resection in patients with clinical stage IA adenocarcinoma of the lung. Eur J Cardiothorac Surg 25:1102–1106
27. Matsunaga T, Suzuki K, Takamochi K, Oh S (2017) What is the radiological definition of part-solid tumour in lung cancer? Eur J Cardiothorac Surg 51:242–247
28. Asamura H, Hishida T, Suzuki K et al (2013) Radiographically determined noninvasive adenocarcinoma of the lung: survival outcomes of Japan Clinical Oncology Group 0201. J Thorac Cardiovasc Surg 146:24–30
29. Suzuki K, Koike T, Asakawa T et al (2011) A prospective radiological study of thin-section computed tomography to predict pathological noninvasiveness in peripheral clinical IA lung cancer (Japan Clinical Oncology Group 0201). J Thorac Oncol 6:751–756